JOURNAL of
MATERIALS and MECHATRONICS:A

e-ISSN 2717-8811
JournalMM, 2026, 7(1), 122-133
https://doi.org/10.55546/jmm.1945970

Araştırma Makalesi / Research Article

Surface Plasmon Resonance Nanosensor Development for Imidacloprid Detection Using Molecularly Imprinting Polymer

Bahar BANKOĞLU YOLA*

* Gaziantep Islam Science and Technology University, Faculty of Engineering and Natural Sciences, Department of Engineering Basic Sciences, Gaziantep, Türkiye,
ORCID ID: https://orcid.org/0000-0002-2931-077X, bahar.bankogluyola@gibtu.edu.tr

Geliş/ Received: 06.05.2026; **Revize/Revised:** 15.05.2026 **Kabul / Accepted:** 22.06.2026

ABSTRACT: Imidacloprid (IMI) is an extensively used neonicotinoid insecticide, widely applied for effective pest control in various crops, as well as for the management of seed and soil pests. Monitoring IMI levels can provide important contamination risks, inform regulatory decisions regarding pesticide use, and guide strategies aimed at mitigating adverse environmental consequences. In this study, we focused on developing a surface plasmon resonance (SPR) nanosensor for IMI detection. Our initial step involved modifying the gold surface of the SPR chip. This was achieved through the self-assembly of allylmercaptane to form a monolayer, thus introducing polymerizable double bonds onto the chip's surface. After that, IMI imprinted poly(2-hydroxyethylmethacrylate–methacryloylamidoglutamicacid) [p(HEMA–MAGA)] film was designed on gold surface of SPR chip. The surfaces, both non-modified and IMI-imprinted p(HEMA–MAGA), were characterized using some analytical techniques, including atomic force microscopy (AFM), fourier transform infrared (FTIR) spectroscopy, and ellipsometry. The developed SPR nanosensor demonstrated a linear detection range between 1.0 ng L^{-1} and 10.0 ng L^{-1} and accomplished a limit of detection (LOD) as low as 0.33 ng L^{-1} and finally applied to the drinking water samples with high recovery.

Keywords: Imidacloprid, Surface plasmon resonance, Molecularly imprinting polymers, Application

*Sorumlu yazar / Corresponding author: bahar.bankogluyola@gibtu.edu.tr
Bu makaleye atıf yapmak için /To cite this article

Bankoğlu Yola, B. (2026). Surface plasmon resonance nanosensor development for ımidacloprid detection using molecularly imprinting polymer. *Journal of Materials and Mechatronics: A, 7*(1), 122-133.

1. INTRODUCTION

IMI represents a novel class of compounds characterized by its strong affinity for insect acetylcholine receptors (Nicholson et al., 2024). IMI, extensively used across numerous crops, raises concerns regarding its potential residues in agricultural products and the environment. It can contaminate waterways through runoff, negatively affecting aquatic invertebrates and potentially accumulating in the food chain. There's also growing concern about its persistence in soil and water, leading to long-term exposure for various ecosystems. For humans, while direct acute toxicity is considered low, chronic exposure risks and potential impacts on neurological development are areas of ongoing scientific investigation and concern. (Sriapha et al., 2020; Tomizawa & Casida, 2005). Currently, the detection of these IMI residues relies on some traditional analytical techniques such as fluorescence method (Wang et al., 2025), high-performance liquid chromatography (HPLC) (Baskaran et al., 1997; Daghi et al., 2025; Fernandez-Alba et al., 1996) and gas chromatography-mass spectrometry (GC-MS) (Navalón et al., 1997; Vilchez et al., 1996). Despite their accuracy, these instrumental methods are often quite costly and time-consuming due to the extensive sample preparation and cleanup processes. Developing rapid and selective analytical method is crucial for the early diagnosis of metabolic disorders. Among these analytical techniques available, SPR sensors are useful due to their compatibility with microfluidic systems. This compatibility is particularly advantageous in the creation of integrated "lab-on-a-chip" platforms combining sample handling, chemical analysis, and data processing within a singular and compact device (Mayer & Hafner, 2011). Furthermore, SPR sensors provide the superior capability for real-time and simultaneous evaluation of both molecular association and dissociation processes (Chen & Ming, 2012). Thus, SPR-based sensor systems have extensive applications in food analysis (Mavioğlu Kaya et al., 2026). Their efficiency and versatility make them important analytical tools in modern analytical chemistry.

Molecular imprinting is an advanced polymer fabrication strategy in a three-stage process (Abrão et al., 2014). Initially, the functional monomers engage with the target molecule through covalent and/or non-covalent interactions, suggesting the formation of a critical pre-polymerization complex (Schirhagl, 2014). This complex then is subjected to the polymerization, providing the molecular recognition sites. Following the polymerization process, the template molecule is extracted with a suitable solvent, which in turn yields highly selective polymeric matrices. These molecularly imprinted polymers (MIPs) have numerous benefits, such as straightforward synthesis, economical production, exceptional selectivity, and impressive physicochemical resilience. Thus, MIPs based sensors have been used for food safety analysis (Baggiani et al., 2007; Ramström et al., 2001). Especially, food safety is a complex domain, requiring rapid, accurate, and often on-site detection of various contaminants and quality indicators. MIPs offer several compelling benefits that make them ideal for this application. MIP-based sensors are being developed and applied to detect a wide array of substances (pesticide, antibiotic residues, toxins and quality control markers) critical for ensuring food safety and quality (Huang et al., 2011; Liang et al., 2016; Xu & Lu, 2016). This research introduced an innovative methodology for the accurate detection of IMI pesticide, leveraging the unique capabilities of MIPs. The core of this research initiated with the simple self-assembled monolayer formation of MIPs. This technique aimed for a thin, uniform, and highly accessible imprinted layer, maximizing binding site availability and minimizing mass transport limitations. Subsequently, this advanced MIPs was integrated into an SPR chip via spin coating process. It was a widely used method for depositing thin, uniform polymer films and allowed for precise control over film thickness and homogeneity, which was crucial for SPR applications where film thickness directly impacted sensitivity and signal stability. This resulting SPR nanosensor demonstrated successful

application in accurately quantifying IMI concentrations within drinking water samples, contributing to the scientific literature. This could pave the way for more accessible pesticide monitoring tools, advancing environmental analysis and public health protection.

2. MATERIALS AND METHODS

2.1. Chemicals and Instrumentation

Permethrin (PERM), parathion (PAR), thiamethoxam (THIA), carbendazim (CAR), allyl mercaptane (CH_2CHCH_2SH), MAGA, ethylene glycol dimethacrylate (EGDMA), HEMA, N,N′-azobisisobutyronitrile (AIBN), phosphate buffer (0.1 mol L^{-1}, PB) and sodium chloride (NaCl) were purchased by Sigma-Aldrich (USA).

FTIR (Bruker Optics Inc., Ettlingen, Germany), nano magnetics instrument mode AFM (Tokyo, Japan), and auto-nulling imaging ellipsometer (Nanofilm EP3, Germany) were used for the structural characterizations and the observation of surface thicknesses. SPR system (GenOptics, SPRi-Lab, Orsay, France) was used for analytical applications.

2.2. CH_2CHCH_2SH Modification of SPR Chip and The Development of IMI Imprinted SPR Chip Cased on CH_2CHCH_2SH

Initially, SPR chips underwent a primary cleaning phase by being submerged for 10 min via an acidic piranha solution (a 3:1 volumetric ratio of H_2SO_4:H_2O_2). Following this, the chips were carefully dried using an argon atmosphere to protect against potential degradation. Afterwards, to establish a robust gold-sulfur interaction, a suspension of CH_2CHCH_2SH, at a concentration of 10.0 mg mL^{-1}, was applied directly onto the gold surface of every SPR chip. The resulting modified chips (designated as CH_2CHCH_2SH/SPR) were stored under an argon atmosphere, ready for their intended experimental applications. The process of fabricating the IMI-imprinted SPR chip, utilizing CH_2CHCH_2SH, commenced with the precise preparation of a MAGA-IMI complex solution. This critical solution was created by combining MAGA and IMI in a 2:1 molar ratio within 10.0 mL of PB, carefully maintained at a pH of 6.0. A polymerization mixture was prepared by combining 5.0 mL of the complex solution with 2.0 mg of AIBN, 10.0 mL of HEMA, and 10.0 mL of EGDMA. This carefully formulated mixture was then applied to the CH_2CHCH_2SH/SPR chip using a 10 min spin coating process. This application method was crucial for ensuring the formation of a uniform, single-layered polymeric structure on the chip's surface. Spin coating allowed for very precise control over the thickness of the MIPs film deposited on SPR chip. This was critical because film thickness directly influenced sensor parameters. Because thinner films often meaned shorter diffusion distances for the IMI target molecule to reach the binding sites, it caused faster response times and potentially higher sensitivity. In addition, the consistent film thickness across multiple sensor devices was crucial for ensuring reproducible sensor performance, and reliable data. The imprinting sequence was finished with UV polymerization applied for 15 min directly onto the SPR chip, thereby successfully generating the IMI-imprinted SPR chip. For UV polymerization, a mercury vapor lamp served as the primary light source, providing a broad emission spectrum across the ultraviolet range. This lamp delivered wavelengths spanning from 315 nm to 400 nm, with adjustable intensity of 10 to 100 mW cm^{-2}. For the purpose of comparative analysis, a control IMI-nonimprinted SPR chip was also developed. This control chip adhered to an identical fabrication protocol, with the exclusion of the IMI target molecule during its preparation.

2.3. IMI Removal from IMI-imprinted p(HEMA–MAGA)/SPR Chip and Analysis Process

To ensure the thorough elimination of electrostatic interactions between the MAGA monomer and the IMI analyte, the IMI-imprinted p(HEMA–MAGA)/SPR chip underwent a crucial immersion step. For 10 min, the chip was submerged in 10.0 mL of a 0.1 mol L^{-1} NaCl solution, a process vital for achieving complete desorption of the IMI molecules. After IMI analyte binded to IMI-imprinted SPR chip, it occupied the specific recognition site. For the sensor to be used again, these sites were effectively cleared. In addition, the ability to reuse a sensor multiple times significantly reduced the cost per analysis. If IMI analyte could not desorb, each measurement required a new SPR sensor chip, making it impractical for many applications. Reusable sensors are also more environmentally friendly, as they generate less waste compared to single-use alternatives. After this essential desorption, the IMI-imprinted p(HEMA–MAGA)/SPR with IMI removal was subjected to vacuum-drying.

After the IMI-imprinted chip integration into the SPR cell, an initial equilibration phase involving 3.0 mL of pH 6.0 solution for 10 min was carried out. The initial equilibration phase referred to the period during which the MIPs based sensor was allowed to stabilize in the measurement environment before the actual detection of the IMI analyte. This solvent/pH stabilization was also crucial for establishing a stable baseline signal before IMI analyte introduction. Hence, this ensured that only the IMI analyte could cause a specific SPR signal during the actual measurement. Following this equilibration, the adsorption phase commenced utilizing various IMI amount solutions. Each individual adsorption solution was permitted to interact with the IMI-imprinted p(HEMA–MAGA)/SPR chip for 40 min. Effective adsorption occurred when the IMI analyte fitted precisely into these binding sites, forming stable interactions. This was the essence of the "lock and key" mechanism employed by MIPs to selectively recognize their target. The adsorption of the IMI analyte to the MIPs caused a detectable change in some physicochemical property of the sensor layer. For instance, in optical sensors, adsorption could lead to a change in refractive index, or absorbance. Then, the desorption phase commenced with the introduction of 3.0 mL of a 0.1 mol L^{-1} NaCl solution for 10 min. This systematic approach ensured that a comprehensive "adsorption–desorption–regeneration" cycle was consistently executed for every tested IMI amount.

2.4. Sample Preparation

For analyzing drinking water samples, a 5.0 mL aliquot was initially placed into a 25.0 mL conical flask. To eliminate any solid residues, this sample underwent centrifugation for 5 min, yielding a clear supernatant. This supernatant was then finally diluted with PB at pH 6.0, a critical step performed to ensure the IMI concentration within the optimal linear range of the SPR system.

3. RESULTS AND DISCUSSION

3.1. Characterization

Upon the elimination of IMI, FTIR spectroscopy, which was applied to IMI-imprinted p(HEMA–MAGA) film/SPR nanosurface, depicted distinctive absorption peaks (Figure 1A). A pronounced band at 3616 cm^{-1} was specifically attributed to the hydroxyl stretching vibration of MAGA, while the hydroxyl stretching of HEMA was located at 3049 cm^{-1}. Additionally, the stretching of –CH bonds was clearly indicated by a band positioned at 1749 cm^{-1}, and an absorption band at 1459 cm^{-1} signified both the carboxyl-carbonyl stretching and the characteristic –COO–

stretching. The collective presence of these distinct spectral bands confirmed the successful development of the IMI-imprinted SPR nanoplatform.

Ellipsometry measurements were additionally conducted, showing a clear harmony with AFM data. The observed surface depth of the IMI-imprinted SPR nanosurface was determined to be 19.79±0.89 nm (Figure 1B). For many polymer films formed via methods like spin-coating or self-assembly, this thickness range was often indicative of a well-controlled, single-layer formation rather than multi-layered growth or disorganized bulk deposition. The harmony with AFM data suggested an absence of significant three-dimensional aggregation.

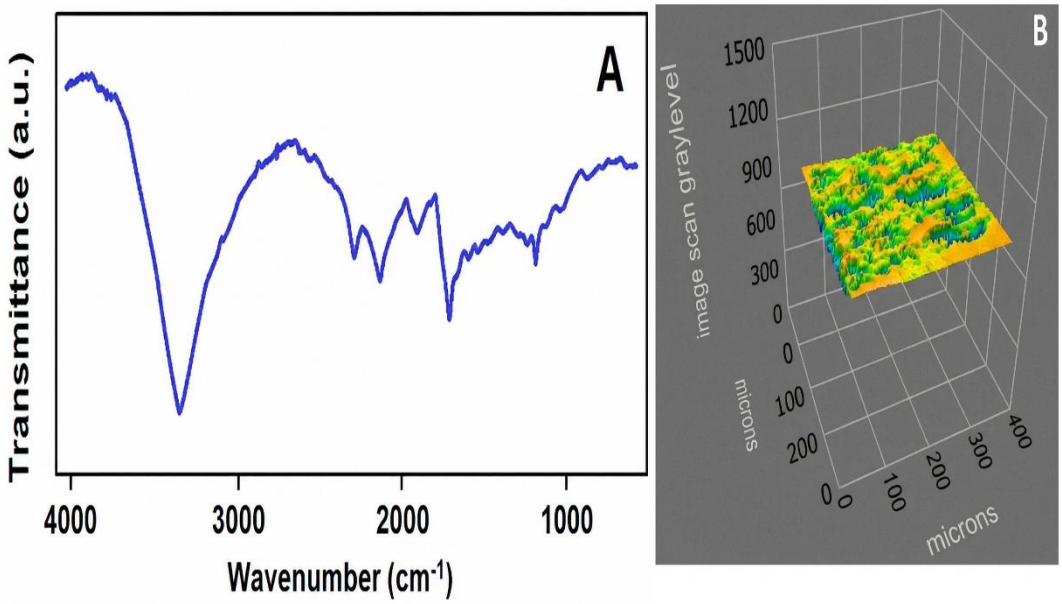

Figure 1. (A) FTIR spectra of IMI-imprinted SPR nanosurface with IMI removal and (B) ellipsometry image of IMI-imprinted SPR nanosurface

AFM images of the SPR surfaces were obtained using the non-contact mode (Figure 2). Especially, the unmodified SPR chips showed a surface depth of 4.89±0.12 nm. This value reflected the inherent roughness and morphology of the gold film. Gold films, depending on their deposition method (e.g., sputtering, evaporation), often exhibited nanoscale grain structures and associated roughness. Following modification with CH_2CHCH_2SH, the surface depth increased to 9.73±0.81 nm. Thiol molecules were well-known to form strong dative bonds with gold surfaces, typically leading to the formation of self-assembled monolayers (SAMs). Finally, the IMI-imprinted p(HEMA–MAGA) film deposited onto CH_2CHCH_2SH-modified SPR chip demonstrated a surface depth of 19.91±1.07 nm. This magnitude of thickness was entirely consistent with the successful deposition of a thin polymer film. Copolymers like p(HEMA–MAGA) could form dense films, and a thickness in the range of 10−20 nm was typical for surface-grafted or spin-coated polymer layers designed for biosensing applications. Finally, these measurements provided important insights into the changes occurring at the SPR surface after each modification step.

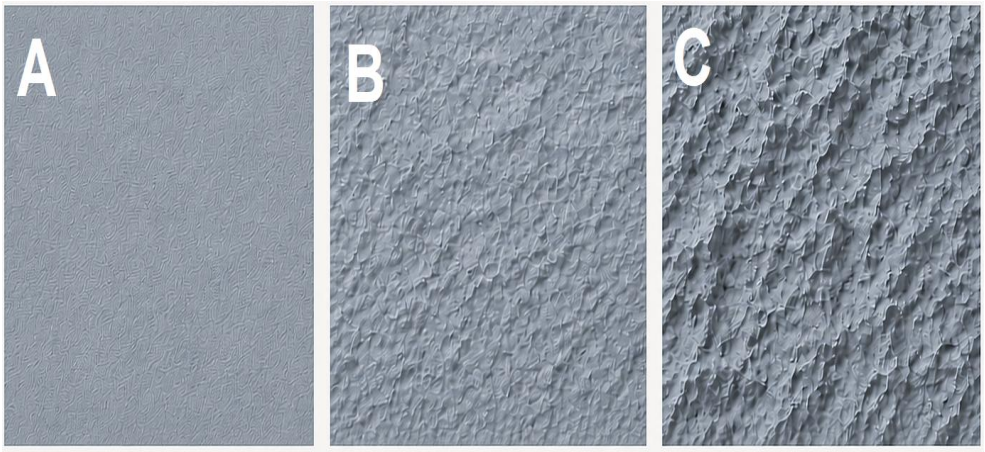

Figure 2. AFM images of (A) nonmodified; (B) CH_2CHCH_2SH modified; (C) IMI-imprinted p(HEMA–MAGA) film/SPR nanosurface

3.2. pH Effect on SPR Signals Using IMI-imprinted p(HEMA–MAGA) Film/SPR Nanosensor

The pH level played a critical role in the terms of the interaction between the acidic MAGA monomer and the IMI analyte. The interaction between the MAGA monomer and IMI was profoundly influenced by pH. Given that the MAGA monomer had two distinct dissociation constants (pKa1=2.10 and pKa2=4.07), its ionization was notably suppressed in acidic environments, leading to a restricted interaction with IMI. As the pH increased, the carboxylic acid functionalities within the MAGA monomer was subjected to deprotonation, resulting in negatively charged groups. These anionic sites then facilitated an enhanced interaction with the −NH groups present in IMI. Conversely, at pH levels exceeding 7.0 (alkaline conditions), the increased prevalence of IMI's anionic form caused a reduction in the monomer-IMI interaction. This observed decrease was primarily ascribed to the enhanced electrostatic repulsion, which consequently decreased their binding strength on the SPR chip surface. Consequently, the optimal interaction between the monomer and analyte was identified in a slightly acidic environment, specifically at a pH of 6.0 (Figure 3) (Akıcı et al., 2026).

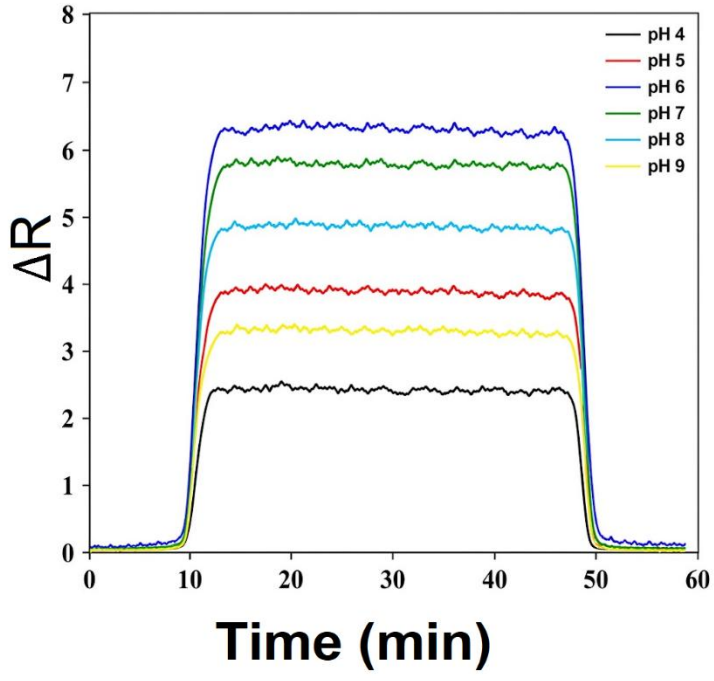

Figure 3. SPR sensorgrams for 5.0 ng L^{-1} IMI in different pHs of PB

3.3. Sensitivity of IMI-imprinted p(HEMA–MAGA) Film/SPR Nanosensor

The performance of the IMI-imprinted p(HEMA–MAGA) film/SPR chip was effectively demonstrated through its analytical functionalities, as evidenced by SPR sensorgrams presented in Figure 4A. These sensorgrams precisely recorded the SPR changes across an IMI concentration spectrum, ranging from 1.0 up to 10.0 ng L^{-1}. This confirmed the SPR chip's ability to accurately detect and quantify IMI within this specified range. A robust linear relationship emerged between the SPR nanosensor signals and the IMI concentration using the calibration equation of $y(\Delta R)=1.0238x(C_{IMI}$, ng $L^{-1})+0.8984$ (Figure 4B). This system exhibited remarkable sensitivity, achieving a limit of quantification (LOQ) of 1.0 ng L^{-1} and a LOD of 0.33 ng L^{-1}. The corresponding equation 1 and equation 2 were given below.

$$LOQ = 10.0\ S / m \quad (1)$$

$$LOD = 3.3\ S / m \quad (2)$$

S: Standard deviation of the intercept and m*:* Slope of the regression line.

The scientific literature indicated that while LC-MS and HPLC techniques were developed for IMI detection (Daghi et al., 2025; Imanzadeh Sarabi et al., 2025), their environmental impact was an important problem owing to extensive chemical usage. Furthermore, these methods were disadvantageous due to their long analysis times and the requirement for highly specialized personnel. In contrast, this study employed a simple self-assembled monolayer formation technique for developing the IMI-imprinted p(HEMA–MAGA) film/SPR, providing minimal waste production and high yield. Consequently, the IMI-imprinted p(HEMA–MAGA) film/SPR system represented a rapid and robust analytical solution for identifying significant metabolic disorders linked to exposure to critical pesticides. In addition, the other significant advantages followings: (i) The "simple self-assembled monolayer formation technique" implied easier fabrication of the sensing element compared to the complex setup and operation of LC-MS/HPLC. (ii) Making IMI testing possible in field settings or production facilities rather than solely in centralized laboratories. (iii) Lower chemical consumption, less specialized labor, and potentially reusable sensor surfaces can lead to significant cost reductions.

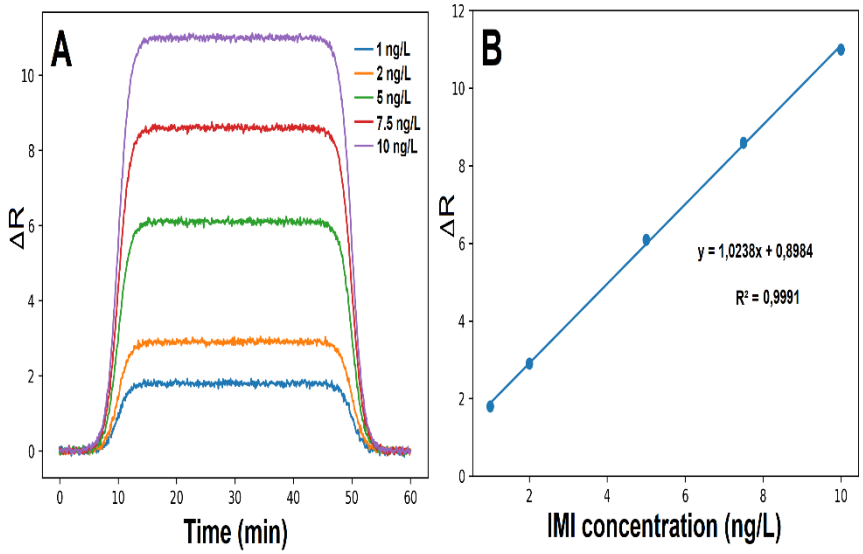

Figure 4. (A) SPR sensorgrams illustrating the response of the IMI-imprinted p(HEMA–MAGA) film/SPR chip to varying IMI concentrations (ranging from 1.0 to 10.0 ng L^{-1} in 6.0 PB solution), and (B) the corresponding calibration curve which plots these IMI concentrations against their respective SPR signals

3.4. Recovery

To thoroughly validate the IMI-imprinted SPR chip, recovery measurements were carried out using drinking water samples. Table 1 illustrated the sensor's outstanding performance, registering a recovery rate of approximately 100.00%. This impressive result underscored the sensor's remarkable precision and its ability to distinguish target analytes effectively in complex matrix interference. For comparative analysis, IMI detection in drinking water sample was also performed using the LC-MS technique (Imanzadeh Sarabi et al., 2025). As shown in Table 1, the results obtained from both the IMI-imprinted SPR chip and the LC-MS methods showed no significant difference. In addition, the findings, as summarized in Table 1, clearly demonstrated a robust agreement between the measurements obtained via the IMI-imprinted p(HEMA–MAGA) film/SPR and the established LC-MS methodology. The statistical analysis, specifically the Wilcoxon test ($T_{calculated}>T_{tabulated}$, $p>0.05$), confirmed the absence of any significant disparity between the results generated by these two distinct approaches, thereby highlighting their strong correlation and interchangeability for the assessed parameters.

Furthermore, the application of the standard addition method to drinking water samples for IMI analysis yielded a calibration equation of $y(\Delta R)=1.0269x(C_{IMI}, \text{ng } L^{-1})+1.3496$. The remarkable agreement observed between the slopes derived from both the direct calibration and standard addition calibration methods provided compelling evidence for the superior specificity of the developed IMI-imprinted p(HEMA–MAGA) film/SPR chip. This strong correlation effectively demonstrated the sensor's capability to maintain its highly selective performance in the presence of diverse matrix interference effects.

Table 1. Recovery results of IMI (*n*=6)

IMI-imprinted p(HEMA–MAGA) film/SPR				LC-MS	
Sample	**Added IMI (ng L^{-1})**	**Found IMI (ng L^{-1})**	***Recovery (%)**	**Found IMI (ng L^{-1})**	***Recovery (%)**
Drinking water	-	0.83 ± 0.04	-	0.84 ± 0.03	-
	2.00	2.84 ± 0.01	100.35 ± 0.02	2.85 ± 0.03	100.35 ± 0.02
	5.00	5.82 ± 0.02	99.83 ± 0.06	5.85 ± 0.05	100.17 ± 0.02
	7.00	7.84 ± 0.03	100.13 ± 0.04	7.83 ± 0.02	99.87 ± 0.03

*Recovery = Found IMI, ng L^{-1} / Real IMI, ng L^{-1}

3.5. Stability, Selectivity, Repeatability, and Reproducibility of IMI-imprinted p(HEMA–MAGA) Film/SPR Nanosensor

IMI-imprinted p(HEMA–MAGA) film/SPR chip exhibited exceptional operational stability over an 8-week assessment. Throughout this stability evaluation, the consistent SPR sensorgrams were obtained using a 5.0 ng L^{-1} IMI. By the close of the eighth week, the recorded SPR signal maintained approximately 98.06% of the initial signal observed after the first week. This performance highlighted the remarkable long-term stability of the developed sensor.

For selectivity of IMI-imprinted p(HEMA–MAGA) film/SPR chip, PERM and PAR were selected as control pesticides present in real samples and THIA and CAR were chosen for the chemical structure similarity with IMI (Pérez-Fernández et al., 2020). The prepared IMI-imprinted SPR chip was effectively utilized for the analysis of various analytes within pH 6.0 PB solution. Specifically, it was applied to a sample containing 5.0 ng L^{-1} IMI, alongside PERM, PAR, THIA, and CAR, as depicted in Figure 5A. According to the calculations of selectivity (k) and relative selectivity

(k') coefficients (Table 2), IMI-imprinted SPR chip determined IMI with increased selectivity, 24.80 times greater than for PERM, 31.00 times greater than for PAR, and 62.00 times greater than for THIA, and 124.00 times greater than for CAR. Figure 5B clearly demonstrated the superior selectivity achieved through molecular imprinting technology, particularly when comparing the performance of the IMI-imprinted SPR chip against its IMI-nonimprinted counterpart. Furthermore, the k' values ranging from 12.40 to 24.80, as detailed in Table 2, suggested the high specificity of the IMI-imprinted SPR chip for targeted IMI detection. This data confirmed the effectiveness of the imprinting process in achieving good selectivity.

Table 2. k and k′ values of IMI-imprinted SPR chip (MIP) and IMI-nonimprinted SPR chip (NIP) (*n*=6)

	MIP		NIP		
	ΔR	**k**	**ΔR**	**k**	**k′**
IMI	6.20 ± 0.02	-	0.10 ± 0.03	-	-
PERM	0.25 ± 0.01	24.80	0.10 ± 0.01	1.00	24.80
PAR	0.20 ± 0.03	31.00	0.05 ± 0.02	2.00	15.50
THIA	0.10 ± 0.04	62.00	0.02 ± 0.01	5.00	12.40
CAR	0.05 ± 0.01	124.00	0.01 ± 0.03	10.00	12.40

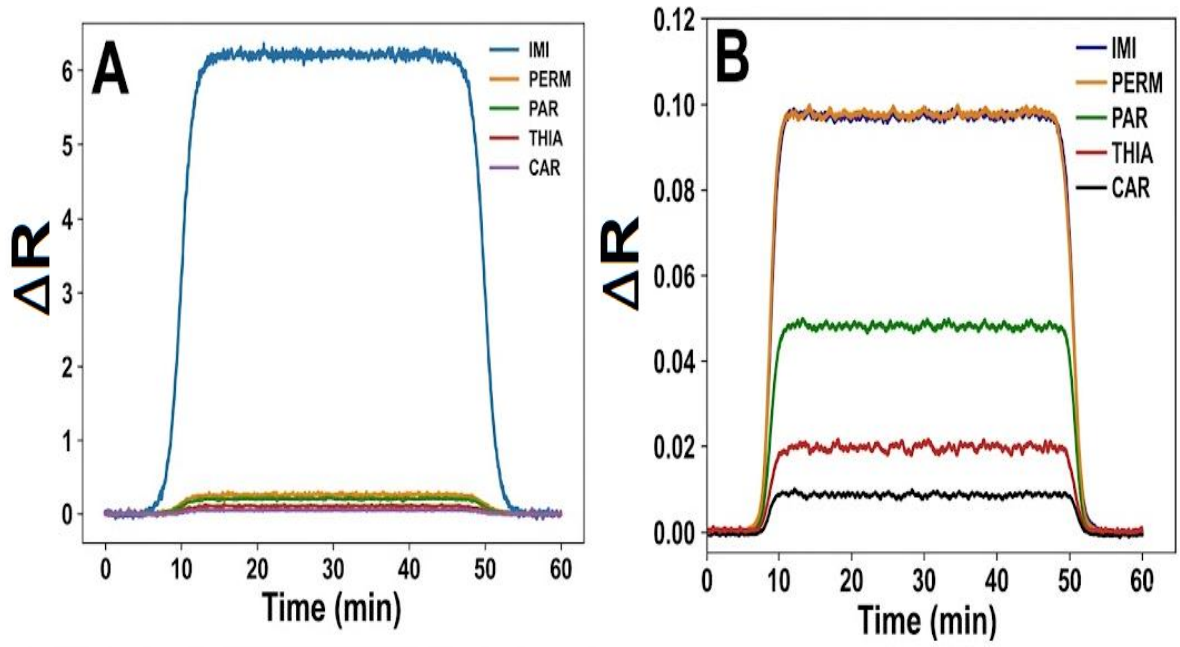

Figure 5. Selectivity studies at (A) IMI-imprinted SPR chip and (B) IMI-nonimprinted SPR chip in 5.0 ng L^{-1} IMI, 5.0 ng L^{-1} PERM, 5.0 ng L^{-1} PAR, 5.0 ng L^{-1} THIA and 5.0 ng L^{-1} CAR

The repeatability of a single IMI-imprinted p(HEMA–MAGA) film/SPR chip was rigorously evaluated by performing five consecutive "adsorption–desorption–regeneration" cycles using a 5.0 ng L^{-1} IMI solution. Across all five cycles, remarkably consistent SPR signals, averaging approximately 6.20 ΔR belonging to a relative standard deviation (RSD) of 0.23%, were consistently recorded (as depicted in Figure 6). This high level of consistency provided compelling evidence for the excellent repeatability of the IMI-imprinted p(HEMA–MAGA) film/SPR chip's performance.

The reproducibility of the sample preparation procedure was thoroughly assessed by fabricating 10 independent IMI-imprinted SPR chips. These 10 independent IMI-imprinted SPR chips were consistently produced in uniform batches, strictly adhering to the methodology detailed in Section 2.2. Following their fabrication, these chips were stored in a sealed environment maintained at 25 °C.

This storage condition was significant to protect the SPR chips from potential fluctuations in temperature and pressure, affecting the integrity and reliability of the devices for subsequent use. Each of these custom-prepared chips was subsequently exposed to a 5.0 ng L^{-1} IMI solution. The SPR signals obtained from these10 distinct chips exhibited a remarkably low relative standard deviation of 0.91%, which strongly affirmed the high level of reproducibility inherent in the developed sample preparation methodology.

3.6. Ruggedness and Robustness of IMI-imprinted p(HEMA–MAGA) Film/SPR Nanosensor

The IMI-imprinted p(HEMA–MAGA) film/SPR nanosensor underwent rigorous evaluation to confirm its reliability, specifically focusing on its ruggedness and robustness, with all comparative statistical analyses conducted via the Wilcoxon test. The ruggedness of the sensor was successfully demonstrated by assessing its performance when different researchers handled the evaluation in the presence of 5.0 ng L^{-1} IMI solution, where the observed lack of a statistically significant difference ($p>0.05$) underscored its operational stability regardless of the operator. Furthermore, the IMI-imprinted p(HEMA–MAGA) film/SPR nanosensor's robustness was established by examining the effects of slight variations from the ideal pH — specifically at pH 5.9 and pH 6.1 — on the analytical results and the absence of any notable statistical deviation ($p>0.05$) in these results confirmed the sensor's strong robustness to minor fluctuations in environmental conditions.

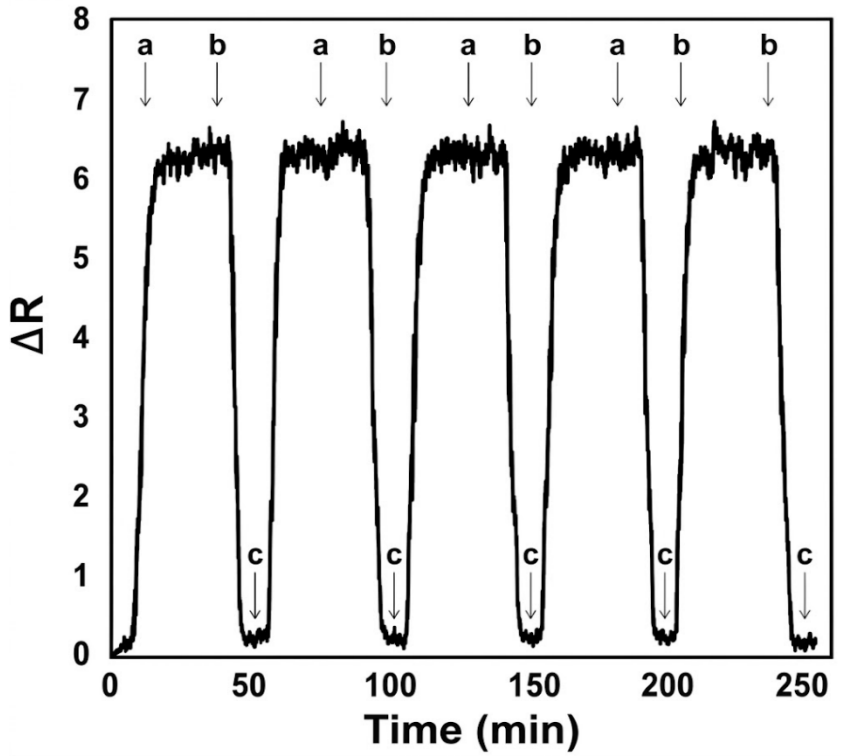

Figure 6. Repeatability of IMI-imprinted p(HEMA–MAGA) film/SPR chip: (a) adsorption; (b) desorption; (c) regeneration

4. CONCLUSION

A novel molecularly imprinted SPR nanosensor was developed for IMI determination in drinking water samples. Some analytical features such as the stability, selectivity, sensitivity, reproducibility and repeatability of the prepared SPR nanosensor were evaluated. The sensor

consistently demonstrated a linear detection capability across a range spanning from 1.0 ng L^{-1} to 10.0 ng L^{-1}. Furthermore, it was able to achieve a notably low detection limit of 0.33 ng L^{-1}, making it highly sensitive for the target analyte. Furthermore, the analytical results exhibited excellent recovery rates from 99.83% to 100.35%.

The innovative integration of molecular imprinting technology with SPR detection offers superior selectivity and reusability, making this nanosensor a cost-effective and efficient analytical tool. Beyond its immediate application for IMI, this robust platform holds immense potential for wide-ranging future studies. Its adaptable design suggests that it could be readily re-engineered to target a diverse array of other pesticides and environmental pollutants, thereby revolutionizing environmental monitoring and public health protection. This development not only provides a powerful new instrument for current challenges but also lays a strong foundation for the next generation of highly sensitive and versatile analytical devices.

5. CONFLICT OF INTEREST

Author approves that to the best of their knowledge, there is not any conflict of interest or common interest with an institution/organization or a person that may affect the review process of the paper.

6. AUTHOR CONTRIBUTION

Bahar BANKOĞLU YOLA contributed to the determining and management the concept and/or design process of the reseach, data collection, data analysis and interpretation of the results, preparation of the manuscript, critical analysis of the intellectual content, final approval and full responsibility.

7. REFERENCES

Abrão, L. C. C., Maia, P. P., & Figueiredo, E. C. (2014). Determination of tetracyclines by solid-phase extraction with a molecularly imprinted polymer and high-performance liquid chromatography. *Analytical Letters*, *47*(13), 2183-2194.

Akıcı, Ş. Y., Düzel, A., Alptekin, Ü. M., Bekerecioğlu, S., Polat, İ., Atar, N., & Yola, M. L. (2026). A novel molecular imprinted quartz crystal microbalance sensor for fenamiphos determination based on boron-sulphur co-doping ultra-thin graphitic carbon nitride incorporated Cu-MOF. *Analytical Methods*, *18*(6), 1331-1339.

Baggiani, C., Anfossi, L., & Giovannoli, C. (2007). Solid phase extraction of food contaminants using molecular imprinted polymers. *Analytica chimica acta*, *591*(1), 29-39.

Baskaran, S., Kookana, R. S., & Naidu, R. (1997). Determination of the insecticide imidacloprid in water and soil using high-performance liquid chromatography. *Journal of Chromatography A*, *787*(1-2), 271-275.

Chen, Y., & Ming, H. (2012). Review of surface plasmon resonance and localized surface plasmon resonance sensor. *Photonic Sensors*, *2*(1), 37-49.

Daghi, M. M., Farajzadeh, M. A., Abbasalizadeh, A., Mogaddam, M. R. A., & Abolhasani, J. (2025). Development of continuous fabric phase sorptive extraction imidacloprid and acetamiprid from fruit juice samples using covalent organic frameworks prior to HPLC-MS/MS analysis. *Microchemical Journal*, *208*, 112355.

Fernandez-Alba, A. R., Valverde, A., Agüera, A., Contreras, M., & Chiron, S. (1996). Determination of imidacloprid in vegetables by high-performance liquid chromatography with diode-array detection. *Journal of chromatography A*, *721*(1), 97-105.

Huang, J., Zhang, X., Liu, S., Lin, Q., He, X., Xing, X., & Lian, W. (2011). Electrochemical sensor for bisphenol A detection based on molecularly imprinted polymers and gold nanoparticles. *Journal of Applied Electrochemistry*, *41*(11), 1323-1328.

Imanzadeh Sarabi, B., Afshar Mogaddam, M. R., Farajzadeh, M. A., & Sorouraddin, S. M. (2025). Dispersive solid phase extraction of acetamiprid and imidacloprid from vegetables using quasi-metal organic frameworks before analysis by liquid chromatography-tandem mass spectrometry. *Microchemical Journal*, *210*, 112915.

Liang, C., Wang, H., He, K., Chen, C., Chen, X., Gong, H., & Cai, C. (2016). A virus-MIPs fluorescent sensor based on FRET for highly sensitive detection of JEV. *Talanta*, *160*, 360-366.

Mavioğlu Kaya, M., Deveci, H. A., Bankoğlu Yola, B., Polat, İ., Bekerecioğlu, S., Atar, N., & Yola, M. L. (2026). Molecularly Imprinted Deoxynivalenol Surface Plasmon Resonance Sensor Based on Sulfur-Doped Boron Graphitic Carbon Nitride. *Foods*, *15*(3), 481.

Mayer, K. M., & Hafner, J. H. (2011). Localized surface plasmon resonance sensors. *Chemical Reviews*, *111*(6), 3828-3857.

Navalón, A., González-Casado, A., El-Khattabi, R., Vilchez, J. L., & Fernández-Alba, A. R. (1997). Determination of imidacloprid in vegetable samples by gas chromatography–mass spectrometry. *Analyst*, *122*(6), 579-581.

Nicholson, C. C., Knapp, J., Kiljanek, T., Albrecht, M., Chauzat, M. P., Costa, C., De la Rúa, P., Klein, A.-M., Mänd, M., Potts, S. G., Schweiger, O., Bottero, I., Cini, E., de Miranda, J. R., Di Prisco, G., Dominik, C., Hodge, S., Kaunath, V., Knauer, A., Laurent, M., Martínez-López, V., Medrzycki, P., Pereira-Peixoto, M. H., Raimets, R., & Rundlöf, M. (2024). Pesticide use negatively affects bumble bees across European landscapes. *Nature*, *628*(8007), 355-358.

Pérez-Fernández, B., Mercader, J. V., Abad-Fuentes, A., Checa-Orrego, B. I., Costa-García, A., & de la Escosura-Muñiz, A. (2020). Direct competitive immunosensor for Imidacloprid pesticide detection on gold nanoparticle-modified electrodes. *Talanta*, *209*, 120465.

Ramström, O., Skudar, K., Haines, J., Patel, P., & Brüggemann, O. (2001). Food analyses using molecularly imprinted polymers. *Journal of Agricultural and Food Chemistry*, *49*(5), 2105-2114.

Schirhagl, R. (2014). Bioapplications for molecularly imprinted polymers. *Analytical Chemistry*, *86*(1), 250-261.

Sriapha, C., Trakulsrichai, S., Tongpoo, A., Pradoo, A., Rittilert, P., & Wananukul, W. (2020). Acute imidacloprid poisoning in Thailand. *Therapeutics and Clinical Risk Management*, 1081-1088.

Tomizawa, M., & Casida, J. E. (2005). Neonicotinoid insecticide toxicology: mechanisms of selective action. *Annual Review of Pharmacology and Toxicology*, *45*(1), 247-268.

Vilchez, J. L., El-Khattabi, R., Fernández, J., González-Casado, A., & Navalón, A. (1996). Determination of imidacloprid in water and soil samples by gas chromatography-mass spectrometry. *Journal of Chromatography A*, *746*(2), 289-294.

Wang, J., Wang, X., Yang, Y., Zhou, X., Dai, Z., Hao, P., Han, G., Yao, J., Yu, X., & Ye, Z. (2025). Dual-readout fluorescence ‘turn-on’lateral flow immunoassay for sensitive detection of imidacloprid. *Biosensors and Bioelectronics*, *279*, 117379.

Xu, S., & Lu, H. (2016). Mesoporous structured MIPs@CDs fluorescence sensor for highly sensitive detection of TNT. *Biosensors and Bioelectronics*, *85*, 950-956.